

Turbulent boundary layer flow subject to streamwise oscillation of spanwise wall-velocity

M. Skote^{a)}

School of Mechanical and Aerospace Engineering, Nanyang Technological University, 50 Nanyang Avenue, Singapore 639798

(Received 13 April 2011; accepted 12 July 2011; published online 19 August 2011)

Direct numerical simulations have been performed to study the effect of a stationary distribution of spanwise wall-velocity that oscillates in the streamwise direction on a turbulent boundary layer. For the first time, a spatially developing flow with this type of forcing is studied. The part of the boundary layer which flows over the alternating wall-velocity section is greatly affected with a drag reduction close to 50% which exhibits an oscillatory distribution with a wavenumber which is twice that of the imposed wall-velocity. The maximum in drag reduction occurs where the wall velocity is at its maximum (or minimum) and the minimum occurs where the wall velocity is zero. Comparisons of the mean spanwise velocity profiles with the analytical solution to the laminar Navier-Stokes equations show very good agreement. The streamwise velocity profile indicates a thickening of the viscous sub-layer when scaled with the local friction velocity and an upward shifting of the logarithmic region when scaled with the reference (unmanipulated) friction velocity. An estimation of the idealized power consumption shows that—with the present wall forcing magnitude—more energy is required for the spatial oscillation than what is saved by drag reduction. © 2011 American Institute of Physics. [doi:10.1063/1.3626028]

Controlling turbulence with the ultimate goal of relaminarization has for a long time been (and still is) an engineer's or scientist's dream. Many control strategies have been investigated in the past, both feedback-control techniques¹ and open-loop in the form of wall motion or body force,² with a varying degree of complicated structure of the control forcing. On the other hand, a number of experimental and numerical studies have shown that a crude oscillation of the wall actually decreases the turbulence significantly, and thus also the viscous drag from the fluid flowing over the wall is reduced.

The first studies of turbulent flows over an oscillating wall were performed numerically using direct numerical simulations (DNS). The geometry of choice in most DNS studies has been either channel^{3–9} or pipe flow,^{5,10–12} while experimental work has concentrated on boundary layers^{13–20} and pipe flow.^{21,22} One exception is the work by Yudhistira and Skote²³ which is the only DNS, so far, on turbulent boundary layer over an oscillating wall.

In most of the numerical work, the wall oscillation is imposed through a wall velocity (W) in the spanwise direction in the form of

$$W = W_m \sin(\omega t), \quad (1)$$

where W_m is the maximum wall velocity and ω is the angular frequency of the wall oscillation, which is related to the period (T) through $\omega = 2\pi/T$.

The oscillation in time may not be practical to implement in an engineering application which has recently lead researchers^{24–26} to consider a steady variation in the streamwise direction along the plate instead of a time-dependent

forcing. In this case, the wall velocity (W) is imposed in the form of

$$W = W_m \sin(\kappa x), \quad (2)$$

where κ is the wavenumber of the spatial oscillation, which is related to the wavelength (λ_x) through $\kappa = 2\pi/\lambda_x$.

The work so far on this type of spatial oscillation has solely been performed using DNS of channel flow by Viotti *et al.*²⁴ Quadrio *et al.*²⁵ have studied (through DNS) the combination of spatial and temporal wall oscillation (stream-wise travelling waves) in a channel flow. However, only marginal improvement on the drag reduction (DR) (compared to the stationary forcing) was obtained. The theoretical and numerical studies were recently further developed by Quadrio and Ricco.²⁶

In the present letter, results are presented from the first investigation of boundary layer flow with a steady spanwise wall velocity which is varying in the streamwise direction according to Eq. (2).

The numerical code and grid are the same as in the previous simulation of an oscillating turbulent boundary layer reported by Yudhistira and Skote,²³ who also showed that the grid is sufficiently fine. The code was developed at KTH, Stockholm.²⁷ A pseudo-spectral method is employed, with Fourier discretization used in the streamwise and spanwise directions, and Chebyshev polynomials in the wall-normal direction. The simulations start with a laminar boundary layer at the inflow which is triggered to transition by a random volume force near the wall. A fringe region is added at the end of the computational domain to enable simulations of spatially developing flows. In this region, the flow is forced from the outflow of the physical domain to the inflow. In this way, the physical domain and the fringe region together satisfy periodic boundary conditions.

^{a)}Electronic mail: mskote@ntu.edu.sg.

All quantities are non-dimensionalized by the freestream velocity (U) and the displacement thickness (δ^*) at the starting position of the simulation ($x=0$), where the flow is laminar. The Reynolds number is set by specifying $Re_{\delta^*} = U\delta^*/\nu$ at $x=0$. In all the simulations presented here, $Re_{\delta^*} = 450$. The computational box is 600 in simulation length units (δ^*) long (including 100 units for the fringe), 30 units high, and 34 units wide.

As the fringe starts at $x=500$, we will present results only up to $x=470$ to avoid any upstream influence of the fringe. The transition region is roughly between $x=5$ and $x=150$. Thus, the region of a fully developed turbulent boundary layer, free from any influence of the numerical method, is $x=150-470$. The Reynolds number based on the momentum thickness (Re_{θ}) is varying between 418 and 750 in this region for the unmanipulated (reference) boundary layer. In inner scaling (based on the friction velocity at $x=250$), the region amounts to about 7200 wall units.

The code has been modified to allow for a streamwise modulation of the spanwise wall-velocity, and the implementation is very similar to the one used by Yudhistira and Skote,²³ except that the wall velocity follows a sinuous distribution in the downstream direction (x) according to Eq. (2) instead of the original time-dependent oscillation described by Eq. (1).

The resolution used for the simulations were 800 modes in streamwise direction, 201 modes in wall-normal direction, and 144 modes in the spanwise direction. This grid size result in a spatial resolution of $\Delta X^+ \times \Delta Z^+ \times \Delta Y^+_{min} = 16 \times 5.1 \times 0.04$. Note that unless otherwise stated, the + superscript indicates that the quantity is made non-dimensional with the friction velocity of the unmanipulated boundary layer (the reference case), denoted u_{τ}^0 , and the kinematic viscosity (ν).

The sampling time for the reference case was 6000 in time units (δ^*/U), started only after a stationary flow (in the statistical sense) was reached. In the case with wall forcing, the total sampling time was 8000.

In the simulation presented here, the maximum wall velocity (W_m) and wavelength (λ_x) are set to 0.857 and 58.17, respectively, which in wall units corresponds to $\lambda_x^+ = 1300$ and $W_m^+ = 17$, based on u_{τ}^0 where the wall forcing starts ($x=250$). The wall forcing is applied between $x=250$ and $x=487.2$ in simulation coordinates, which corresponds to four periods, or a total length of applied wall motion of 5300 in wall units. Note that the wall forcing is of the same magnitude as the freestream velocity ($W_m = 0.857U$) and the flow thus deviates substantially from the unmanipulated boundary layer. Further simulations are needed in order to investigate a much weaker and, hence, more practical wall forcing.

The resulting DR is calculated from

$$DR(\%) = 100 \frac{C_f^0 - C_f}{C_f^0}, \quad (3)$$

where C_f^0 is the skin friction of the reference case and is shown in Fig. 1 (solid line). The downstream development of the DR is similar to the temporal oscillating case²³ (dashed line in Fig. 1). However, the maximum DR is 46% which is

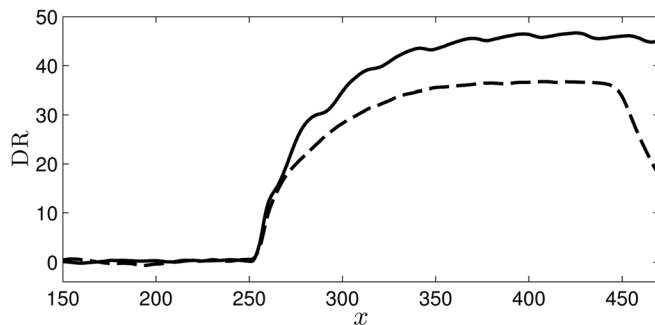


FIG. 1. Downstream development of the drag reduction. (—) spatial forcing; (---) temporal forcing (data taken from Ref. 23). Wall velocity is imposed from $x=250$.

substantially larger than the corresponding DR for the temporal oscillation which is 37%. For the temporal case, the maximum wall velocity was the same ($W_m^+ = 17$), while the period was chosen as $T^+ = 100$. Note that the wall forcing ends at $x=450$ in this case and, hence, the DR reduces from that point. In the channel flow simulation by Viotti *et al.*,²⁴ the maximum DR was reported to be 52% with $\lambda_x^+ = 1250$ and $W_m^+ = 20$.

The qualitative similarity between the response to spatial and temporal forcing, respectively, further strengthen the theory presented by Viotti *et al.*²⁴ that the temporal forcing can be translated to spatial forcing by using a convection velocity of the near-wall turbulence fluctuations (denoted U_w^+) which relates the oscillation period and wave length through $\lambda_x^+ = U_w^+ T^+$. For a direct comparison between the present spatial case and a temporal simulation, T^+ would be set to 130 if the estimated value of $U_w^+ = 10$ found in the literature²⁸ is used.

The spatial oscillation observed in the DR (the solid line in Fig. 1) is statistically stationary and correlates with the wall velocity oscillation. To further investigate, the DR taken from two equal time intervals (4000 each in simulation units, which corresponds to about 4500 in viscous units) are shown in Fig. 2 together with the wall velocity (with a value of 40 added in order to fit in the scale of the figure). The difference in DR from the two intervals is at most 1.5% which indicates that the DR is statistically converged. The phase and amplitude remain the same for the two intervals which demonstrate that the oscillation of the DR is not a transient phenomenon. The DR exhibits an oscillatory distribution with a wavenumber which is twice of the wall-velocity. When comparing the DR with the wall velocity oscillation, it becomes

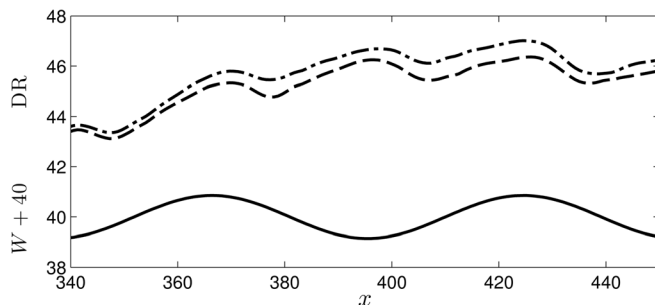


FIG. 2. Drag reduction statistics from two equal time intervals (---) and (- · -). Wall velocity $W+40$ (—).

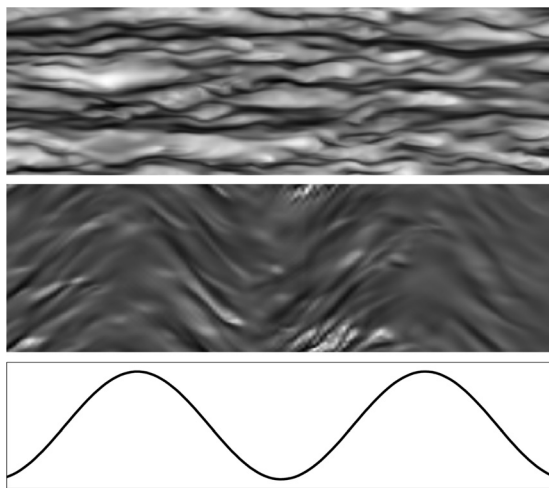


FIG. 3. Instantaneous velocity fields in a plane parallel to the wall at a distance $y = 0.5$, corresponding to $y^+ = 11$ (based on u_τ^0) from the unmanipulated boundary layer (top) and the oscillating case (middle) forced with the wall velocity distribution (bottom). The dark gray indicates low-speed regions and lighter shades indicate high-speed patches. In viscous units, the part shown is 770 wide and 2500 long. The flow is from left to right.

apparent (Fig. 2) that the maximum in DR occurs where the wall velocity is at its maximum (or minimum) and that the minimum in DR is correlated to the positions where the wall velocity is zero.

Some insight into the oscillating behavior of the DR can be obtained by studying a snapshot of the turbulent velocity field. In Fig. 3, the streamwise velocity fluctuations in the unmanipulated boundary layer are shown in the top figure. The streamwise extent is the same as in Fig. 2, while the whole spanwise width of the computational domain is shown. The long streaky low-speed regions are clearly visible (the darker shaded areas in Fig. 3). The same domain is shown for the oscillating case in the middle figure together with the wall-velocity distribution in the bottom figure. The low-speed streaks are disappearing in the region corresponding to maximum and minimum wall velocity and reappear (albeit oblique) around the parts where the wall velocity is zero. Hence, the maximum DR coincides with the weakening of turbulence structures and the minimum in DR corresponds to the reappearance of low-speed streaks.

The streamwise velocity profile at $x = 424$ is shown in viscous scaling in Fig. 4. The velocity profile scaled with the actual u_τ follows the linear profile ($u^+ = y^+$) close to the wall. A thickening of the viscous sub-layer is observed (compared to the reference velocity profile). This was also observed in the channel flow²⁴ profiles. The thickening is larger in actual (physical) y -coordinates since u_τ is lower in the reference case.

When the same velocity profile is scaled with u_τ^0 , the profile collapses with the reference profile in the outer region. In the small (due to the low Reynolds number) logarithmic region, the profile is shifted upward in the wall forcing case.

The Reynolds stresses behave in the same way as reported from the temporal case.²³ However, the maximum decreases even further by 39%, 29%, and 52% for the longitudinal (rms-value), normal (rms-value), and shear Reynolds

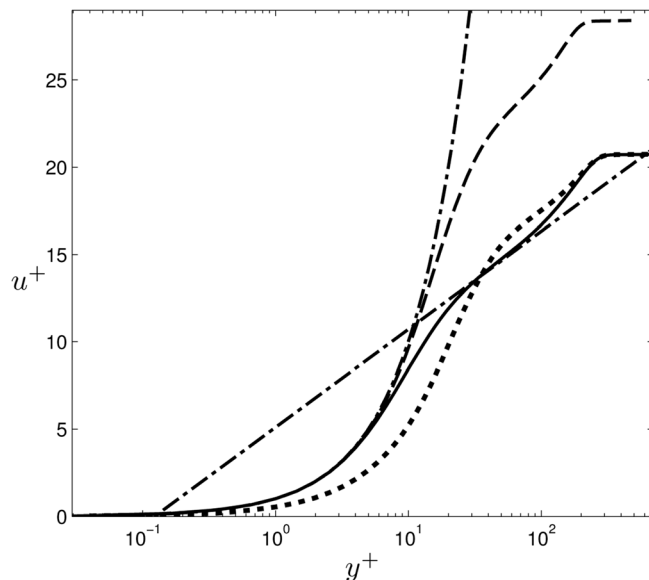


FIG. 4. Velocity profile at $x = 424$. (—) unmanipulated boundary layer; (---) wall forcing case scaled with actual u_τ ; (···) wall forcing case scaled with u_τ^0 ; (- · -) $u^+ = y^+$, and $u^+ = \frac{1}{0.41} \ln y^+ + 5.1$.

stresses, respectively, while the corresponding values from Ref. 23 were 33%, 22%, and 40%.

From channel flow simulations,²⁴ the near-wall spanwise velocity profiles were reported to follow the analytical solution to the laminar Navier-Stokes equations. The analytical solution was derived^{24,26} using the assumption of a thin spatial Stokes layer (SSL) and may be written as

$$w(x, y) = C_x \Re \left[\exp(ikx) \text{Ai} \left(-\frac{iy}{\delta_x} e^{-i4/3\pi} \right) \right], \quad (4)$$

where C_x is a normalization constant and $\kappa = 2\pi/\lambda_x$ is the forcing wave number. Ai is the Airy function and the thickness of the SSL is described by

$$\delta_x = \left(\frac{\nu^2 \lambda_x}{u_\tau^2 2\pi} \right)^{1/3}. \quad (5)$$

Note that δ_x varies downstream in a boundary layer flow unlike in the channel flow geometry. Expressed in wall units, Eq. (5) can be written as $\delta_x^+ = (\lambda_x^+ / 2\pi)^{1/3}$. We also note in Eq. (4) that the x -coordinate is scaled with κ and the y -coordinate is scaled with δ_x and thus we can form the non-dimensional vertical coordinate $\eta = y/\delta_x$.

The profiles from Eq. (4) are compared with the DNS data at three points where the wall velocity is at its maximum and minimum levels, and zero, respectively. As the results in Fig. 5 indicate, the overlap is very good. Thus, even in the boundary layer flow, where the flow is inhomogeneous in the downstream direction, the spanwise velocity profile follows the prediction derived from the laminar equations.

Lastly, the energy saving due to DR is compared to the energy required to move the wall by estimating the idealized power consumption, following the derivation by Quadrio *et al.*²⁵ and extended to boundary layer flow. The percentage saved power P_{sav} is equal to the percentage of friction DR

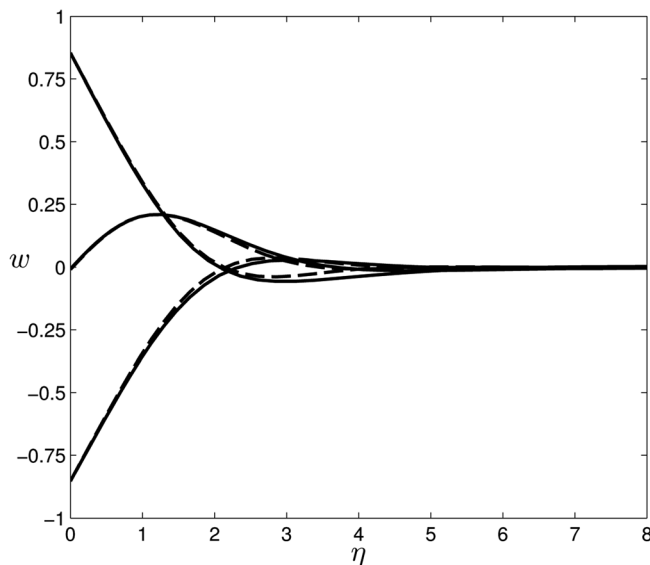


FIG. 5. Spanwise velocity profiles from three points where the wall velocity is at its maximum and minimum levels, and zero, respectively. (—) DNS; (- -) from Eq. (4). Note that the mirror image for the zero velocity profile is omitted.

(Eq. (3)), and integrated over a distance with approximately constant DR and integer number of periods (in this case $x = 340\text{--}456$). The required percentage power P_{req} is similarly defined in terms of the friction power of the reference flow and may be written as

$$P_{req} = \int \nu \frac{\partial w}{\partial y} \Big|_{y=0} W dx \Big/ \int (u_{\tau}^0)^2 U dx. \quad (6)$$

The net percentage power saving is defined as $P_{net} = P_{sav} + P_{req}$ and is calculated to be -19% for the case presented here. Thus, the power needed to drive the wall in the spanwise direction is greater than the power saved by streamwise DR. These results are consistent with the channel flow simulations²⁵ which indicate a P_{net} of -35% for a similar κ as in the present investigation and with $W_m^+ = 12$. The results presented by Viotti *et al.*²⁴ showed that P_{net} becomes positive (up to 23%) for lower amplitudes of the forcing ($W_m^+ = 6$). Future simulations will hopefully confirm that the trend is similar for the turbulent boundary layer flow.

¹N. Kasagi, Y. Suzuki, and K. Fukagata, "Microelectromechanical systems-based feedback control of turbulence for skin friction reduction," *Annu. Rev. Fluid Mech.* **41**, 231 (2009).

²G. E. Karniadakis and K. S. Choi, "Mechanisms on transverse motions in turbulent wall flows," *Annu. Rev. Fluid Mech.* **35**, 45 (2003).

- ³W. J. Jung, N. Mangiavacchi, and R. Akhavan, "Suppression of turbulence in wall-bounded flows by high-frequency spanwise oscillations," *Phys. Fluids A* **4**, 1605 (1992).
- ⁴A. Baron and M. Quadrio, "Turbulent drag reduction by spanwise wall oscillations," *Appl. Sci. Res.* **55**, 311 (1996).
- ⁵J. I. Choi, C. X. Xu, and H. J. Sung, "Drag reduction by spanwise wall oscillation in wall-bounded turbulent flows," *AIAA J.* **40**, 842 (2002).
- ⁶M. Quadrio and P. Ricco, "Initial response of a turbulent channel flow to spanwise oscillation of the walls," *J. Turbul.* **4**, 7 (2003).
- ⁷M. Quadrio and P. Ricco, "Critical assessment of turbulent drag reduction through spanwise wall oscillations," *J. Fluid Mech.* **521**, 251 (2004).
- ⁸C. X. Xu and W. X. Huang, "Transient response of reynolds stress transport to spanwise wall oscillation in a turbulent channel flow," *Phys. Fluids* **17**, 018101 (2005).
- ⁹P. Ricco and M. Quadrio, "Wall-oscillation conditions for drag reduction in turbulent channel flow," *Int. J. Heat Fluid Flow* **29**, 601 (2008).
- ¹⁰M. Quadrio and S. Sibilla, "Numerical simulation of turbulent flow in a pipe oscillating around its axis," *J. Fluid Mech.* **424**, 217 (2000).
- ¹¹A. Duggleby, K. S. Ball, and M. R. Paul, "The effect of spanwise wall oscillation on turbulent pipe flow structures resulting in drag reduction," *Phys. Fluids* **19**, 125107 (2007).
- ¹²J. Fang and L. Lu, "Large Eddy simulation of compressible turbulent channel flow with active Spanwise wall fluctuations," *Mod. Phys. Lett. B* **24**, 1457 (2010).
- ¹³F. Laadhari, L. Skandaji, and R. Morel, "Turbulence reduction in a boundary layer by a local spanwise oscillating surface," *Phys. Fluids* **6**, 3218 (1994).
- ¹⁴S. M. Trujillo, D. G. Bogard, and K. S. Ball, "Turbulent boundary layer drag reduction using an oscillating wall," AIAA Paper No. 97-1870, 1997.
- ¹⁵K. S. Choi, J. R. DeBisschop, and B. R. Clayton, "Turbulent boundary-layer control by means of spanwise wall oscillation," *AIAA J.* **36**, 1157 (1998).
- ¹⁶K. S. Choi and B. R. Clayton, "The mechanism of turbulent drag reduction with wall oscillation," *Int. J. Heat Fluid Flow* **22**, 1 (2001).
- ¹⁷K.-S. Choi, "Near-wall structure of turbulent boundary layer with spanwise-wall oscillation," *Phys. Fluids* **14**, 2530 (2002).
- ¹⁸G. M. Di Cicca, G. Iuso, P. G. Spazzini, and M. Onorato, "Particle image velocimetry investigation of a turbulent boundary layer manipulated by spanwise wall oscillations," *J. Fluid Mech.* **467**, 41 (2002).
- ¹⁹P. Ricco and S. Wu, "On the effects of lateral wall oscillations on a turbulent boundary layer," *Exp. Therm. Fluid Sci.* **29**, 41 (2004).
- ²⁰P. Ricco, "Modification of near-wall turbulence due to spanwise wall oscillations," *J. Turbul.* **5**, 24 (2004).
- ²¹K. Choi and M. Graham, "Drag reduction of turbulent pipe flows by circular-wall oscillation," *Phys. Fluids* **10**, 7 (1998).
- ²²F. Auteri, A. Baron, M. Belan, G. Campanardi, and M. Quadrio, "Experimental assessment of drag reduction by traveling waves in a turbulent pipe flow," *Phys. Fluids* **22**, 115103 (2010).
- ²³I. Yudhistira and M. Skote, "Direct numerical simulation of a turbulent boundary layer over an oscillating wall," *J. Turbul.* **12**, 9 (2011).
- ²⁴C. Viotti, M. Quadrio, and P. Luchini, "Streamwise oscillation of spanwise velocity at the wall of a channel for turbulent drag reduction," *Phys. Fluids* **21**, 115109 (2009).
- ²⁵M. Quadrio, P. Ricco, and C. Viotti, "Streamwise-travelling waves of spanwise wall velocity for turbulent drag reduction," *J. Fluid Mech.* **627**, 161 (2009).
- ²⁶M. Quadrio and P. Ricco, "The laminar generalized Stokes layer and turbulent drag reduction," *J. Fluid Mech.* **667**, 135 (2011).
- ²⁷M. Chevalier, P. Schlatter, A. Lundbladh, and D. S. Henningson, "Simson—A pseudo-spectral solver for incompressible boundary layer flows," Technical Report TRITA-MEK 2007:07, KTH, Stockholm, Sweden, 2007, ISBN 978-91-7178-838-2.
- ²⁸J. Kim and F. Hussain, "Propagation velocity of perturbations in turbulent channel flow," *Phys. Fluids A* **5**, 695 (1993).